Fragility analysis of nonproportionally damped inelastic MDOF structural systems exposed to stochastic seismic excitation

Ioannis P. Mitseas[1*], Michael Beer[1,2,3]

[1]Institute for Risk and Reliability,
Faculty of Civil Engineering and Geodetic Science
Leibniz University Hannover,
Callinstr. 34, 30167, Hannover, Germany
e-mail: *mitseas@irz.uni-hannover.de, beer@irz.uni-hannover.de

[2]Institute for Risk and Uncertainty and School of Engineering,
University of Liverpool,
Peach Street, Liverpool L69 7ZF, UK

[3]International Joint Research Center for Engineering Reliability and Stochastic Mechanics,
Tongji University,
No. 1239, Si Ping Rd. Shanghai 200092, China

Abstract

A novel methodology for conducting efficiently fragility analysis considering nonproportionally damped inelastic multi degree-of-freedom (MDOF) structural systems subject to stochastic seismic excitations defined by an advanced stochastic model consistent with magnitude-epicentral distance earthquake properties is developed. To this aim, an approximate stochastic dynamics technique for determining the system response amplitude probability density functions (PDFs) is developed. Firstly, relying on statistical linearization and state-variable formulation the complex eigenvalue problem is addressed through the time-domain. Secondly, utilizing the forced vibrational modal properties of the linearized MDOF system in conjunction with a combination of deterministic and stochastic averaging treatment, the MDOF system modal response amplitude process PDFs are determined. The modal participation factors are then defined for the complex-valued mode shapes and the total response amplitude process PDFs are provided in physical coordinates. Subsequently, appropriate limit states are related with the higher order statistics of the engineering demand parameters (i.e. that of the PDF) for quantifying structural system related fragilities. Nevertheless, due to the vector-valued nature of the adopted intensity measure, depicting system fragilities takes the form of three-dimensional fragility surfaces. The associated low computational cost renders the proposed methodology particularly useful for efficient structural system fragility analysis and related performance-based engineering design applications. A multi-storey building structure comprising the bilinear hysteretic model serves as a numerical example for demonstrating the reliability of the proposed fragility analysis methodology. Nonlinear response time-history analysis involving a large ensemble of compatible accelerograms is conducted to assess the accuracy of the proposed methodology in a Monte Carlo-based context.

Keywords: fragility surfaces, nonlinear stochastic dynamics, stochastic field, statistical linearization, stochastic averaging, bilinear MDOF hysteretic system

1 INTRODUCTION

Most structures and civil infrastructure systems are subject to excitations, such as earthquakes and winds, which exhibit strong variability in both the intensity and the frequency content (e.g. [1,2]). Clearly, this feature necessitates a careful consideration of the representation for this class of loads by rendering appropriately to the concept of stochastic fields. Next, regarding the transmission of random vibration, the classical damping assumption [3] which has found widespread application in structural engineering practice, can actually be seen as an attribute which constitutes a limitation for any approach that makes use of it. As in most real systems of engineering interest the modal equations of motion are coupled (e.g. [4,5]), it arises naturally that non-classically damped systems are more appropriate to be considered for approaches with broader applicability and versatility. Further, linear time-invariant models are appealing for many structural engineering applications. Nevertheless, in several cases structural components are expected to exhibit nonlinear behaviour associated, in general, either with material or geometrical aspects. In this regard, structural systems under severe earthquake excitations can become nonlinear and inelastic (i.e. plastic/hysteretic) with

restoring forces depending on the response history [6,7]. Note in passing that contemporary aseismic code provisions dictate a ductile behavior under the design seismic action. Since the number of nonlinear random vibration problems that lend themselves to exact solutions is strikingly limited, the predominant approach for determining, with any preselected level of accuracy, the response/reliability statistics and fragilities of nonlinear structural systems under stochastic excitation is the Monte Carlo simulation (MCS) method. However, MCS can be computationally prohibitive, especially in cases where complex nonlinear multi degree-of-freedom (MDOF) systems are considered.

The emerging concept of performance-based engineering (PBE) advocates the assessment of the structural system performance in a comprehensive and rigorous manner by properly accounting for the presence of uncertainties (e.g. [8,9]). Specifically, inherent in the philosophy of the PBE is the definition, in general, of excitation related variables, known as intensity measures (IMs) (e.g., peak ground acceleration, spectral acceleration, etc), and of system response related variables known as engineering demand parameters (EDPs) (e.g., inter-story drift ratio, peak story drifts, etc). Moreover, the information provided via the functional relationship between the IMs and the EDPs in conjunction with appropriately defined damage/limit states (LS), is utilized for quantifying a selected decision variable (e.g., risk of financial loss, life cycle-cost, etc). Nevertheless, determining the above-mentioned functional relationship, and generating system fragilities (i.e. probabilities of exceeding specified damage states given an IM value), constitutes typically a computationally demanding and cumbrous task.

In this regard, it can be argued that there is a need for developing approximate analytical and/or numerical techniques for determining efficiently the response and the associated fragilities of nonlinear structural systems subject to stochastic excitations. Nevertheless, although there is a considerable body in the literature referring to the development of such stochastic response determination techniques (e.g., [5,6,10]) there are limited results related to utilizing such techniques for efficient fragility analysis applications. An interesting contribution in this regard is the work by Der Kiureghian and Fujimura placed in 2009 [11] where an efficient tail-equivalent linearization based approach is applied for fragility analysis of a nonlinear building structure. Furthermore, Kafali and Grigoriu [12] perform structural system fragility analysis utilizing the crossing theory for the cases of linear and nonlinear SDOF oscillators, introducing interestingly alternative intensity measures. Lastly, it is of interest the work of Tubaldi et al. [8] where a combination of analytical and simulation techniques is employed to assess fragilities for adjacent steel buildings connected by viscous dampers.

This paper proposes an efficient fragility analysis methodology which encompasses a novel inelastic modal decomposition method for random vibration analysis in alignment with specifications prescribed by an advanced point source stochastic seismological model for determining the probability law of the induced ground motion considering non-classically damped and nonlinear MDOF systems. Relying on statistical linearization and state-variable formulation the complex eigenvalue problem is addressed through the time-domain. Next, utilizing the forced vibrational modal properties of the linearized MDOF system in conjunction with a combination of deterministic and stochastic averaging treatment, the MDOF system

modal response amplitude process PDFs are determined. The modal participation factors are evaluated for the complex-valued mode shapes and the total response amplitude process PDFs are defined in physical coordinates. Lastly, appropriate LS are related with the higher order statistics of the EDPs (i.e. the PDF) for assessing system related fragilities at a low computational cost.

The proposed fragility analysis methodology differs, as compared with a typically applied fragility analysis implementation, in the following three aspects: (i) the ground motion is modeled in the form of a non-stationary stochastic field rather than a suite of scaled real earthquake records; (ii) instead of the commonly employed scalar IMs of the peak ground acceleration (PGA) or spectral acceleration, a vector-valued IM consisting of two parameters, namely the earthquake moment magnitude M_m and the epicentral distance r (i.e. the distance from the epicentre to system site), is employed; the location dependency renders the considered stochastic field also non-homogeneous in space (in addition to being non-stationary in time); (iii) an efficient approximate nonlinear stochastic dynamics technique is developed for determining efficiently higher order statistics of the EDPs (i.e. the response PDF) and the associated system fragilities; thus, circumventing computationally cumbersome MCS. This latter attribute is of particular importance since it enables methodology to account for *nonlinear MDOF* structural systems liberated from any dependency on the form of damping (i.e. proportionally and nonproportionally damped systems).

In the remainder of this paper Sections 2.1-2.5 review the mathematical background supporting the proposed framework, Section 2.6 furnishes pertinent comments on important attributes and practical usage of the implementation technique, Section 3, presents an illustrative application of the framework to a yielding multi-storey building frame exposed to stochastic seismic excitation and assesses its accuracy against nonlinear response time-history analysis (RHA) data, and Section 4 summarizes the main conclusions.

2 MATHEMATICAL BACKGROUND

This section elucidates the mathematical details involved in the development of the proposed efficient fragility analysis methodology. Particular attention has been given on exemplifying the various simplifications and assumptions made in support of numerical efficiency.

2.1 *Determination of the probability law of the induced seismic action*

The stochastic seismological model proposed by Boore [2] is utilized in the herein study to determine the radiation spectrum and the associated time envelope function. At this point, it is deemed appropriate to note that the choice of the seismological model is not binding and that the proposed methodology can readily be modified to account for provisions and specifications defined by various stochastic seismological models (e.g. [13,14]).

The employed point source seismological model is characterized primarily by the radiation spectrum $Y(\omega; M_m, r)$ and the envelope function $e(t; M_m, r)$, where ω denotes the angular frequency expressed in rad/s whereas M_m and r stand for the moment magnitude and epicentral distance respectively. Specifically, the radiation spectrum $Y(\omega; M_m, r)$ of the ground motion at

a site can be construed as the composition of several contributions from various factors such as the earthquake source (E), the path (P), the site (G), and the type of motion (I)

$$Y(\omega; M_m, r) = E(\omega, M_0)\, P(\omega, r)\, G(\omega)\, I(\omega) \quad (1)$$

where the equivalent two point-source spectrum developed by Atkinson and Silva [15] is employed for the earthquake source in the form

$$E(\omega, M_0) = C\, M_o \left[\frac{1-\varepsilon}{1+(\omega/\omega_a)^2} + \frac{\varepsilon}{1+(\omega/\omega_b)^2}\right]. \quad (2)$$

where M_0 stands for the seismic moment (in dyna-cm) (e.g. [16]) and is related with the moment magnitude M_m according to $M_o = 10^{1.5(M_m+10.7)}$ [17]. Next, the constant C which appears in Eq.(2) is given by the relationship

$$C = \frac{R_\Phi V F}{4\pi R_o \rho_s {\beta_s}^3} \quad (3)$$

where R_Φ is the average radiation pattern, V is a coefficient to account for the partition of waves into two horizontal components, F is the free surface amplification; β_s and ρ_s are the shear-wave velocity and density in the vicinity of the seismic source, and R_o is a reference distance. The lower and upper corner angular frequencies ω_a and ω_b in Eq.(2) are estimated by the corresponding relationships concerning ordinary frequencies which read $\log_{10} f_a = 2.181 - 0.496 M_m$ and $\log_{10} f_b = 2.410 - 0.408 M_m$. The weighting parameter ε is provided by the expression $\log_{10}\varepsilon = 0.605 - 0.255 M_m$. Further, the path component of the process that affects the radiation spectrum of ground motion at a particular site is given by

$$P(\omega, r) = \frac{1}{R}\exp(-\pi\omega R/Q(\omega)\beta_s), \quad (4)$$

where $R = \sqrt{h^2 + r^2}$ is the radial distance from the earthquake source to the site, with h representing a moment dependent, nominal pseudo-depth (in km), given by the expression $\log_{10} h = 0.15 M_m - 0.05$. The employed regional quality factor is given by $Q(\omega) = 680\, \omega^{0.38}$. Next, the modification of seismic waves by local site conditions is considered through the expression

$$G(\omega) = \exp(-\pi k_o \omega)\, A_m, \quad (5)$$

where k_o is a constant; and A_m is a near-surface amplification factor described via empirical curves for generic rock sites. In the ensuing analysis, it is assumed that A_m is equal to a constant value (e.g. [18]). The filter $I(\omega)$ is provided in the following form

$$I(\omega) = (2\pi\omega)^n. \quad (6)$$

Next, considering the acceleration as the utilized type of ground motion yields n equals to two; zero and one correspond to ground displacement and velocity, respectively. In Fig. 1a, the radiation spectra for various values of moment magnitude M_m and a constant value of the epicentral distance r are plotted.

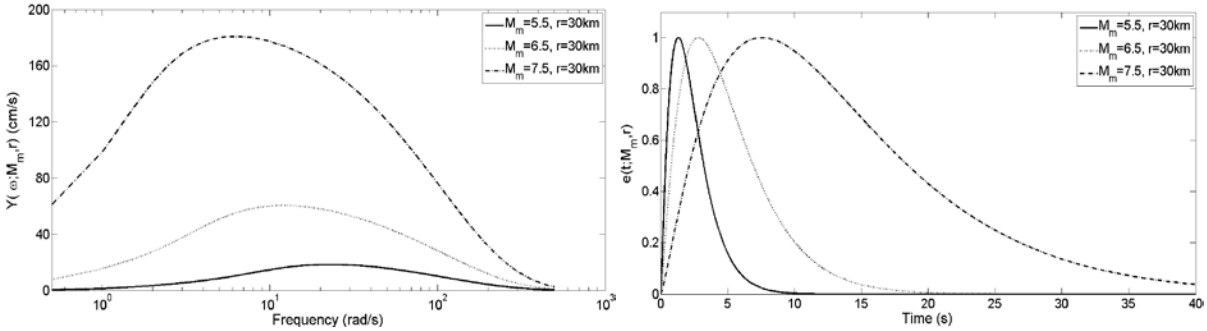

Fig. 1. (a) Radiation spectrum $Y(\omega; M_m, r)$ for various values of M_m and a constant value of $r = 30$km. (b) Envelope function $e(t; M_m, r)$ for various $M_m$values and $r = 30$km; $R_\Phi = 0.55, V = 1/\sqrt{2}$, F = 4, $\beta_s = 3.5$km/s, $\rho_s = 2.8$g/cm^3, $k_o = 0.015$, $A_m = 2.5$ and $n = 2$, $\lambda = 0.2$, $\eta = 0.05$.

Subsequently, the time envelope function $e(t; M_m, r)$ is defined according to the relation

$$e(t; M_m, r) = \alpha(t/t_n)^b \exp\left(-c(t/t_n)\right), \tag{7}$$

with $b = -\lambda\ln(\eta)/[1 + \lambda(\ln(\lambda) - 1)]$, $c = b/\lambda$, $\alpha = [\exp(1)/\lambda]^b$, and $t_n = 0.1R + 2\pi/\omega_a$. Indicatively, in Fig. 1b, the corresponding time envelope functions are provided. Note that the herein point-source stochastic ground motion model has found applicability on a number of structural reliability studies in the field of earthquake engineering (e.g. [18-20]).

In the herein study, based on the findings associated with the employed point source seismological model, meaning the radiation spectrum and the time envelope function, evolutionary power spectra are introduced as functions of moment magnitude and epicentral distance. In this setting, the following relation is proposed

$$S_{\ddot{\alpha}_g}(\omega, t) = |e(t; M_m, r)|^2 Y(\omega; M_m, r). \tag{8}$$

providing a statistical description of the underlying non-stationary in time and non-homogenous in space stochastic field. For illustration purposes, Figs. 2a-b show evolutionary power spectra as well as typical associated realizations of the ground acceleration stochastic process for the site and earthquake conditions depicted in Fig. 1.

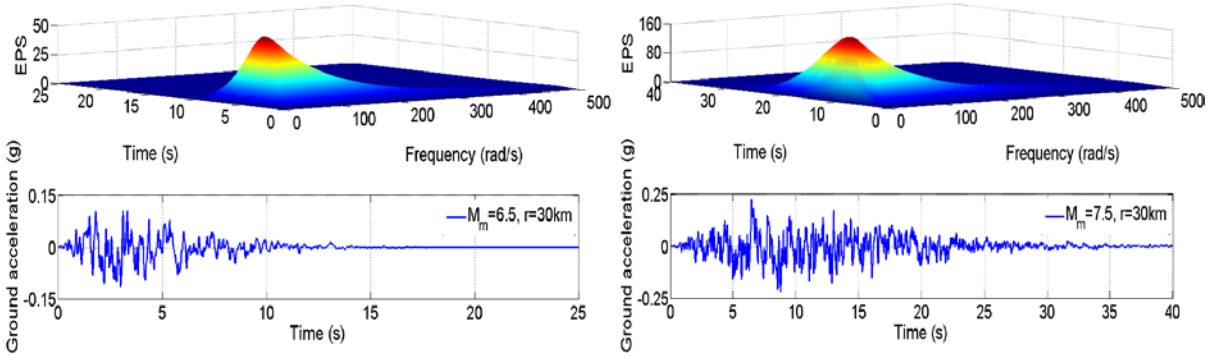

Fig. 2. Evolutionary power spectra and compatible time-realizations of the underlying stochastic processes of the ground motion for (a) $M_m = 6.5$ and $r = 30$km, and (b) $M_m = 7.5$ and $r = 30$km.

Note in passing that the above determined power spectra characterizing the underlying stochastic processes for specific magnitude-epicentral distance earthquake properties are introduced and used as a first numerical step to represent the seismic input action.

2.2 *Statistical linearization for nonproportionally damped nonlinear MDOF systems*

Consider a nonproportionally damped, nonlinear structural system with *n* number of DOFs base-excited by the Gaussian acceleration stochastic process $\ddot{\alpha}_g(t)$, characterized in the frequency domain by the power spectrum $S_{\ddot{\alpha}_g}(\omega, t)$. The dynamic behavior of the structure is governed by the system of differential equations written in vector-matrix form as

$$\mathbf{M}\ddot{\mathbf{y}}(t) + \mathbf{C}\dot{\mathbf{y}}(t) + \mathbf{K}\mathbf{y}(t) + \mathbf{g}\big(\mathbf{y}(t), \dot{\mathbf{y}}(t)\big) = \mathbf{F}(t) = -\mathbf{M}\boldsymbol{\gamma}\ddot{\alpha}_g(t) \tag{9}$$

where $\mathbf{y}(t)$, $\dot{\mathbf{y}}(t)$, and $\ddot{\mathbf{y}}(t)$ denote the response displacement, velocity, and acceleration vectors defined in relative coordinates. Specifically, $y_j(t)$ stands for the inter-story drift $y_j(t) = x_j - x_{j-1}$, whereas x_j for $j = 0,1,2,\dots,n$ is the lateral floor displacement relative to the ground displacement with x_0=0; alternatively, it can be defined as $y_j(t) = \boldsymbol{w}^T\boldsymbol{x}$, where the $1 \times n$ transformation vector $\boldsymbol{w}^T$ for the case of the top floor relative displacement takes the values $[1\ -1\ 0\ \dots\ 0]$; see also [21]. Further, $\mathbf{M}$, $\mathbf{C}$, and $\mathbf{K}$ denote the $(n \times n)$ real-valued mass, damping, and stiffness matrices, respectively while $\boldsymbol{\gamma}$ is a unit $(n \times 1)$ column vector; $\mathbf{g}\big(\mathbf{y}(t), \dot{\mathbf{y}}(t)\big)$ is a nonlinear $n \times 1$ vector function of the variables $\mathbf{y}(t)$ and $\dot{\mathbf{y}}(t)$, used to model the inelastic response of the seismically excited yielding structure.

For nonproportionally damped systems which do not satisfy Caughey and O'Kelly identity [3] meaning cases where $\mathbf{CM^{-1}K} \neq \mathbf{KM^{-1}C}$ the eigenvalues as well as the modal shapes are expected to be complex-valued. Note in passing that the Rayleigh form of damping where the damping matrix is defined to be proportional to the mass and stiffness matrices is a sub-case of Caughey and O'Kelly's identity. Relying on the standard assumption that the response processes are Gaussian, and following statistical linearization [6,22], a linearized version of Eq. (9) is considered in the form

$$\mathbf{M}\ddot{\mathbf{y}}(t) + \big(\mathbf{C} + \mathbf{C_{eq}}\big)\dot{\mathbf{y}}(t) + \big(\mathbf{K} + \mathbf{K_{eq}}\big)\mathbf{y}(t) = \mathbf{F}(t) = -\mathbf{M}\boldsymbol{\gamma}\ddot{\alpha}_g(t), \tag{10}$$

where $k_{je} = k_j + k_{jj}^{eq}$ and $c_{je} = c_j + c_{jj}^{eq}$ with the $(d,l)^{th}$ element of the equivalent linear matrices $\mathbf{C_{eq}}$ and $\mathbf{K_{eq}}$ to be determined by the following expressions

$$c_{d,l}^{eq} = E\left[\frac{\partial g_d}{\partial \dot{y}_l}\right], \qquad k_{d,l}^{eq} = E\left[\frac{\partial g_d}{\partial y_l}\right], \tag{11}$$

in which $E[\cdot]$ is the mathematical expectation operator. A state vector $\mathbf{z}(t)$ can be defined as

$$\boldsymbol{z}(t) = [\mathbf{y}(t) \quad \dot{\mathbf{y}}(t)]^T. \tag{12}$$

In terms of $\mathbf{z}(t)$, the linearized equation of motion Eq.(10) can be written as a first-order matrix equation

$$\dot{\boldsymbol{z}}(t) = \boldsymbol{G}\boldsymbol{z}(t) + \boldsymbol{f}(t) \tag{13}$$

where

$$\boldsymbol{G} = \begin{bmatrix} \mathbf{0} & \boldsymbol{I} \\ -\mathbf{M^{-1}}\big(\mathbf{K} + \mathbf{K_{eq}}\big) & -\mathbf{M^{-1}}\big(\mathbf{C} + \mathbf{C_{eq}}\big) \end{bmatrix} \tag{14}$$

and

$$\boldsymbol{f}(t) = \begin{bmatrix} \mathbf{0} \\ \mathbf{M^{-1}F}(t) \end{bmatrix} \tag{15}$$

The equivalent eigenvalues $\lambda_1^{eq}, \bar{\lambda}_1^{eq}, \ldots \lambda_n^{eq}, \bar{\lambda}_n^{eq}$ of the 2n × 2n matrix $\boldsymbol{G}$ can be computed by solving $|\boldsymbol{G} - \boldsymbol{\lambda I}| = \mathbf{0}$. For a dynamically exited *n*-DOF system, there are *n* pairs of eigenvalues $\lambda_i^{eq}, \bar{\lambda}_i^{eq}$, and to each such pair corresponds a complex conjugate pair of eigenvectors $\boldsymbol{\psi}_i^{eq}, \bar{\boldsymbol{\psi}}_i^{eq}$, with $i = 0,1,2, \ldots,$ n. The equivalent complex modal matrix $\boldsymbol{T^{eq}}$ which is formed as

$$\boldsymbol{T^{eq}} = \left[\boldsymbol{\psi}_1^{eq}, \bar{\boldsymbol{\psi}}_1^{eq}, \ldots \boldsymbol{\psi}_n^{eq}, \bar{\boldsymbol{\psi}}_n^{eq}\right] \tag{16}$$

serves as an appropriate transformation matrix mapping physical to modal coordinates. In this setting, the following transformations are introduced $\boldsymbol{z}(t) = \boldsymbol{T^{eq}}\boldsymbol{u}(t)$ and $\boldsymbol{g}(t) = (\boldsymbol{T^{eq}})^{-1}\boldsymbol{f}(t)$ where the elements of the transformed state vector $\boldsymbol{u}(t)$ can be determined using the convolution integral relationship

$$u_i(t) = \int_0^t exp\left(\lambda_i^{eq}\theta\right) g_i(t-\theta) d\theta \tag{17}$$

where the impulse response function is defined as $h_i(t) = exp\left(\lambda_i^{eq} t\right)$ for $t > 0$. Further, of particular interest from a reliability assessment perspective is the time instant where the excitation spectrum reaches its most critical value, i.e. the $\mathrm{t_{cr}}$ when $\mathrm{e(t; M_m, r)}$ takes its highest value; this attribute enables the ensuing stochastic analysis to focalize on specified values of $\mathrm{t_{cr}}$ dictated by the magnitude-epicentral distance properties where the underlying stochastic seismic processes can be assumed to be locally stationary in time. The correlation matrix of the applied forces $\boldsymbol{f}(t)$ in physical coordinates is given in the form

$$\boldsymbol{R_f}(\tau) = E\{\boldsymbol{f}(t)\boldsymbol{f}^T(t+\tau)\} = \begin{bmatrix} \mathbf{0} & \mathbf{0} \\ \mathbf{0} & \boldsymbol{R_F}(\tau) \end{bmatrix} \tag{18}$$

where $\boldsymbol{R_F}(\tau)$ is defined as the inverse Fourier transform of the applied forces power spectrum matrix which reads in the frequency domain

$$\mathbf{S_F}(\omega, t) = \mathrm{S_{\ddot{a}_g}}(\omega, \mathrm{t})\mathbf{M}\boldsymbol{\gamma}\boldsymbol{\gamma}^{\boldsymbol{T}}\mathbf{M}. \tag{19}$$

Subsequently, the following transformation relation is used

$$\boldsymbol{R_g}(\tau) = (\boldsymbol{T^{eq}})^{-1}\boldsymbol{R_f}(\tau)\ ((\boldsymbol{T^{eq}})^{-1})^{*\mathrm{T}}. \tag{20}$$

where the superscript (*) denotes Hermitian transposition. In the general case of a linear/linearized MDOF system under stochastic excitation a matrix input-output correlation relationship of the form (e.g. [5])

$$R_{u_{dl}}(\tau) = \int_0^\infty \int_0^\infty h_d(\theta_1) R_{g_{dl}}(\tau + \theta_1 - \theta_2) h_l^*(\theta_2)\, d\theta_1 d\theta_2 \tag{21}$$

can be derived, utilizing the convolution integral relationship of Eq.(17). Next, the transformation

$$\boldsymbol{R_z}(\tau) = \boldsymbol{T^{eq}}\boldsymbol{R_u}(\tau)\ \boldsymbol{T^{eq}}^{*\mathrm{T}} \tag{22}$$

can be utilized. The diagonal elements of the response correlation matrix computed at the origin (i.e. $\tau = 0$) provide with estimates of the mean square of the response state vector $\mathbf{z}(t)$.

In the field of aseismic engineering the bilinear hysteretic force-deformation law, shown in Fig. 3b, consists a commonly employed model to capture the hysteretic behavior of structural members and systems under seismic excitation (e.g. [23]). For the case of a bilinear hysteretic oscillator the nonlinear vector function takes the form (e.g. [5,24])

$$g_j\left(\mathrm{y}_j(t),\dot{\mathrm{y}}_j(t)\right) = \alpha_j y_j(t) + \left(1-\alpha_j\right)\sigma_j(t), \tag{23}$$

with the auxiliary state $\sigma_j(t)$ defined as

$$\dot{\sigma}_{\mathrm{j}}(\mathrm{t}) = \dot{\mathrm{y}}_j\left\{1 - U\left(\dot{\mathrm{y}}_j(t)\right)U\left(\sigma_j(t)-\mathrm{x}_y\right) - U\left(-\dot{\mathrm{y}}_j(t)\right)U\left(-\sigma_j(t)-\mathrm{x}_y\right)\right\}, \tag{24}$$

where $U(\cdot)$ denotes the Heaviside step function, namely, $U(\beta)=1$ for $\beta \geq 0$, and $U(\beta)=0$ for $\beta < 0$, x_y is the yielding deformation and α_j is the post-yield to pre-yield stiffness ratio. Through a consideration of a free-body diagram for the j-th story, the equation of motion, reads

$$m_j\sum_{i=1}^{j}\ddot{y}_i(t) + c_j\dot{y}_j(t) - c_{j+1}\dot{y}_{j+1}(t) + k_j g_j\left(\mathrm{y}_j(t),\dot{\mathrm{y}}_j(t)\right) - k_{j+1}g_{j+1}\left(\mathrm{y}_j(t),\dot{\mathrm{y}}_j(t)\right) = -m_j\ddot{\alpha}_{\mathrm{g}}(\mathrm{t}) \tag{25}$$

Adopting the assumptions that the response of a viscously damped bilinear hysteretic SDOF oscillator is contained within a narrow band of frequencies and that the PDF of its amplitude process follows a Rayleigh distribution, the equivalent linear parameters are determined (e.g. [7,25])

$$k_{je} = k_j\left\{1 - \frac{8(1-\alpha_j)}{\pi}\int_1^{\infty}\left[u^{-3} + \left(v_j u\right)^{-1}\right](u-1)^{1/2}e^{-u^2/v_j}du\right\}, \tag{26}$$

and

$$\mathrm{c}_{\mathrm{je}} = \mathrm{c}_{\mathrm{j}} + 2\left(\frac{k_j^2 m_j}{k_{je}}\right)^{1/2}\left(1-\alpha_j\right)\left(\pi v_j\right)^{-1/2}erfc({v_j}^{-1/2}), \tag{27}$$

with

$$v_j = \frac{2R_{y_{jj}}(0)}{\mathrm{x}_y^2} = \frac{E\left[{\mathrm{y}_{\mathrm{j}}}^2(t)\right]}{\mathrm{x}_y^2} \tag{28}$$

Note in passing that the cross-correlation terms in the determination of the expressions for the equivalent linear parameters are neglected due to their relatively low contribution. It can be readily seen that Eqs.(13-22) and Eqs.(26-28) constitute a coupled nonlinear system of algebraic equations to be solved iteratively for the system equivalent linear parameters determination. In this setting, a simple iterative while-loop is sufficient to simultaneously satisfy Eqs.(13-22) and Eqs.(26-28) until convergence of the equivalent linear parameters is achieved within a pre-specified tolerance.

2.3 *Stochastic averaging treatment of the equivalent modal oscillators*

Relying on the assumption of light damping (i.e $\zeta_i < 0.1$), it can be argued that every equivalent modal oscillator exhibits a pseudo-harmonic behavior, allowing for the response amplitude process to be modelled as a one-dimensional Markov process. In this regard, the

modal response amplitude envelope $\mathrm{A_i(t)}$ is a slowly varying function with respect to time defined as (e.g. [10,26,27])

$$A_i^2(\mathrm{t}) = u_i^2(t) + \left(\frac{\dot{u}_i(t)}{\omega_i^{eq}}\right)^2 \tag{29}$$

where the equivalent pseudo-undamped natural circular frequency ω_i^{eq} is related with the corresponding pair of eigenvalues $\lambda_i^{eq}, \bar{\lambda}_i^{eq}$ through the following relation $\omega_i^{eq} = \left|\lambda_i^{eq}\right|$. The modal response $u_i(t)$ is described by the equation

$$u_i(t) = A_i(t)\cos\left(\omega_i^{eq} t + \theta_i(t)\right) \tag{30}$$

where $\theta_i(t)$ stands for the phase of the modal response. Next, based on a combination of deterministic and stochastic averaging a first-order stochastic differential equation (SDE) governing each mode response amplitude process $A_i(t)$ takes the form

$$\dot{A}_i(t) = Re(\lambda_i^{eq})A_i(t) + \frac{\pi S_{\ddot{\alpha}_{ii}}(\omega_i^{eq})}{2A_i(t)\left|\lambda_i^{eq}\right|^2} + \frac{\sqrt{\pi S_{\ddot{\alpha}_{ii}}(\omega_i^{eq})}}{\left|\lambda_i^{eq}\right|}\,\eta(t). \tag{31}$$

In Eq.(31), $\eta(t)$ stands for a stationary, zero mean and delta correlated Gaussian white noise process of unit intensity, i.e., $E\big(\eta(t)\big) = 0$; and $E(\eta(t)\eta(t+\tau)) = \delta(\tau)$, with $\delta(\tau)$ being the Dirac delta function. The mode shapes, $\boldsymbol{\varphi}_i^{eq}$ are given by the upper half of the eigenvectors $\boldsymbol{\psi}_i^{eq}$ forming the transformation matrix $\boldsymbol{\Phi^{eq}}$. The diagonal elements of the ground motion acceleration power spectrum matrix in modal coordinates appearing in Eq.(31) are determined

$$\mathbf{S}_{\ddot{\alpha}}(\omega) = (\boldsymbol{\Phi^{eq}})^{-1}\mathrm{S}_{\ddot{\alpha}_g}(\omega, \mathrm{t_{cr}})\boldsymbol{\gamma\gamma^T}((\boldsymbol{\Phi^{eq}})^{-1})^{*\mathrm{T}} \tag{32}$$

whereas the Fokker-Planck (F-P) partial differential equation governing the response amplitude PDF of the Markovian process A_i corresponding to the i-th mode is

$$\frac{\partial}{\partial \mathrm{t}}\mathrm{p(A_i, t)} = \frac{\partial}{\partial \mathrm{A_i}}\left[\left(-Re(\lambda_i^{eq})\mathrm{A_i} - \frac{\pi S_{\ddot{\alpha}_{ii}}(\omega_i^{eq})}{2\mathrm{A_i}\left|\lambda_i^{eq}\right|^2}\right)\mathrm{p(A_i, t)}\right] + \frac{\partial^2}{\partial \mathrm{A_i}^2}\left[\left(\frac{\pi S_{\ddot{\alpha}_{ii}}(\omega_i^{eq})}{2\left|\lambda_i^{eq}\right|^2}\right)\mathrm{p(A_i, t)}\right] \tag{33}$$

Next, Eq.(33) has been shown to admit as solution a Rayleigh distribution [10,28]

$$\mathrm{p(A_i, t)} = \frac{\mathrm{A_i(t)}}{\mathrm{c_i(t)}}\exp\left(-\frac{\mathrm{A_i(t)}^2}{2\mathrm{c_i(t)}}\right). \tag{34}$$

Substituting Eq.(34) into the F-P equation, and manipulating, yields a first-order ordinary differential equation of the form

$$\dot{\mathrm{c}}_\mathrm{i}(\mathrm{t}) = 2Re\big(\lambda_i^{eq}\big)\mathrm{c_i(t)} + \frac{\pi S_{\ddot{\alpha}_{ii}}(\omega_i^{eq})}{\left|\lambda_i^{eq}\right|^2}, \tag{35}$$

to be solved via standard numerical integration schemes. In this regard, the parameter $\mathrm{c_i(t)}$, and therefore the Rayleigh distribution of the modal response amplitude envelope $\mathrm{A_i(t)}$, are efficiently determined at a particularly low computational cost.

2.4 *Modal combination method for equivalent linear and nonproportionally damped systems*

In conceptual alignment with the generalization of classical modal combination rules such as square-root-of-sums-squared and complete-quadratic-combination (e.g. [7,21]), a modal combination method is provided for the determination of real-valued participation factors Γ_{ji} from the complex-valued mode shapes $\boldsymbol{\varphi}_i^{eq}$. The real-valued coefficients a_i and c_i are defined as $a_i = -2Re(\eta_i \bar{\lambda}_i^{eq})$ and $c_i = 2Re(\eta_i)$, where

$$\eta_i = \left(\boldsymbol{w}^T \boldsymbol{\varphi}_i^{eq}\right)\left(\left(\boldsymbol{\varphi}_i^{eq}\right)^T \boldsymbol{M}\boldsymbol{\gamma}\right)\left(-\lambda_i^{eq}\left(\boldsymbol{\varphi}_i^{eq}\right)^T \boldsymbol{M}\boldsymbol{\varphi}_i^{eq} + \left(\lambda_i^{eq}\right)^{-1}\left(\boldsymbol{\varphi}_i^{eq}\right)^T \mathbf{K}\boldsymbol{\varphi}_i^{eq}\right)^{-\mathbf{1}}. \quad (36)$$

In this regard, the modal participation factors which are determined as

$$\Gamma_{ji} = \sqrt{\left(a_i^2 + \left|\lambda_i^{eq}\right|^2 c_i^2\right)} \quad (37)$$

can be used in conjunction with the distributions of the modal response amplitude of Eq.(34). In this regard, the total response amplitude PDFs arise as the outcome of the convolution of the involved distributions multiplied by the associated weighting factor (i.e modal participation factor) corresponding to the participation of every mode in the estimation of the stationary response amplitude PDF $\mathrm{p}(\mathrm{A_j}, \mathrm{t})$ of the j-th DOF of the system. Lastly, in accordance with classical modal analysis, a subset of the total number of modes can selectively be used (i.e. $r = 0,1,2, \ldots, \leq \mathrm{n}$) in the system response determination.

2.5 Limit states for efficient system fragility analysis estimates

In the literature, there is a considerable body of reliability analysis studies where the damage/limit states (LS) are defined in terms of the overall system inelastic deformation or the maximum inter-story drift (e.g., see [29]). In the herein study, the inter-story drift amplitude process PDFs act as the engineering demand parameters (EDPs) for monitoring structural system performance. In the following, it is assumed that the most critical distribution of response amplitude $\mathrm{p}(\mathrm{A_{j,cr}}, \mathrm{t})$ is the one with the most broad-band form yielding the higher failure probabilities considering appropriate LS. Next, the limit state fragility P_{ls} defined as the probability of exceeding a specified level of damage δ_{ls} conditioned upon the earthquake moment magnitude $\mathrm{M_m}$ and the epicentral distance r, is expressed as

$$\mathrm{P}_{ls}\left[\mathrm{A_{j,cr}}(\mathrm{t}) \geq \delta_{ls} = \delta |\ \mathrm{IM}(\mathrm{M_m}, \mathrm{r})\right] = 1 - \int_0^{\delta} \mathrm{p}\left(\mathrm{A_{j,cr}} |\ \mathrm{IM}(\mathrm{M_m}, \mathrm{r})\right) \mathrm{d}\theta \quad (38)$$

A possible mapping between performance requirements and system limit states, expressed in terms of inter-story drift, for a typical multi-story building structure is provided in Table 1.

Table 1. Performance requirements and limit states

Limit States	Inter-story drift δ_{ls} (%)
Moderate structural damage	1.5
Impaired function	3.0
Life safety	5.0
Onset of collapse	9.0

In this setting, structural system fragilities for various LS conditioned upon magnitude-epicentral distance earthquake properties are readily computed.

2.6 Discussion

A discussion on a number of important aspects which concerns advantages, limitations as well as potential practical applications of the proposed framework is herein presented.

Comparing to the state of the art schemes available in the literature, the proposed stochastic dynamics fragility analysis technique exhibits a number of noteworthy attributes such as: (i) it accounts for *nonlinear* and *MDOF* structural systems, following contemporary aseismic code provisions which encourage a ductile behavior under severe seismic action, (ii) it is liberated from any dependency on the form of damping since it addresses cases of *nonproportionally damped* systems which represent the majority of systems of engineering interest (e.g. [30]), (iii) the challenge of selecting and scaling earthquake records is conveniently avoided; note in passing that the above issue remains highly controversial in the relevant literature (e.g., [31,32]), (iv) owing to the vector-valued nature of the employed IM, depicting system fragilities takes the form of three-dimensional fragility surfaces instead of the usually encountered in the literature planar fragility curves, (v) it is considerably less computationally demanding compared to nonlinear RHA for compatible ground motion records, (vi) it furnishes with equivalent linear eigenvalues conditioned upon magnitude-epicentral distance earthquake properties which occur in complex conjugate pairs. The dynamic character of a system can be determined, to a large extent, from the position of these eigenvalues in the complex plane. (vii) the limit state fragilities can be approximated using just the first few modes (primary contributors) that capture the majority of the system energy. This attribute of the proposed methodology could be particularly advantageous for studying large-scale engineering structures such as high-rise buildings that may need a large number of DOFs to be modelled. (viii) it provides with reliable higher order statistics (i.e. PDF) of the selected EDP rather than simple estimates only of the mean and the standard deviation currently being the norm in the literature.

Pertinent remarks should be given regarding the expected level of accuracy since the proposed method in view of efficiency encompasses a number of techniques which bear plausible limitations. The well-reported in the literature accuracy of statistical linearization (e.g. [5,6]) may render the proposed method not sufficiently accurate for cases of particularly low-performing structures. Under such conditions, the stochastic averaging treatment proposed for the equivalent modal oscillators in favor of achieving substantial computational cost reduction may lessen the achieved degree of accuracy; for cases of highly nonlinear behavior the assumption of the equivalent light damping (i.e $\zeta_i^{eq} = -Re(\lambda_i^{eq})/\left|\lambda_i^{eq}\right| < 0.1$) may not be satisfied. Lastly, no restrictions are imposed on the excitation, with the only exception being the Gaussian assumption.

3 ILLUSTRATIVE APPLICATION

In this section the proposed efficient fragility analysis methodology is numerically exemplified by considering a yielding multi-story frame structure subject to stochastic seismic excitation in alignment with specifications prescribed by an advanced point source seismological model. The degree of accuracy of the predicted limit state fragilities is quantified by comparison with pertinent results derived from nonlinear RHA for a large ensemble of time-realizations compatible with the underlying stochastic processes for specific magnitude-epicentral distance earthquake properties.

3.1 Nonproportionally damped inelastic MDOF frame structure

The three-story nonproportionally damped inelastic shear frame shown in Fig. 3a is considered to illustrate the proposed approach. The lumped masses m_j, the stiffness and damping coefficients of the j-th story, k_j and c_j, respectively, are provided as $m_1 = m_2 = m_3 = 60\ ton$, $k_1 = 7.25\ MNm^{-1}$, $k_2 = 4\ MNm^{-1}$, $k_3 = 2\ MNm^{-1}$, $c_1 = 40\ kNsm^{-1}$, $c_2 = 30\ kNsm^{-1}$, and $c_3 = 20\ kNsm^{-1}$. The elastoplastic behavior of the shear frame is governed by a hysteretic relationship between the resisting story shearing force of the j-th story and the corresponding inter-story drift shown in Eqs.(23-24) whereas the yielding displacement x_y is taken equal to $5\ cm$. Lastly, various values of α_j (post-yield to pre-yield stiffness ratio) are assumed in view of studying a range of inelastic behaviors; $\alpha_1 = 0.3$, $\alpha_2 = 0.5$ and $\alpha_3 = 0.7$.

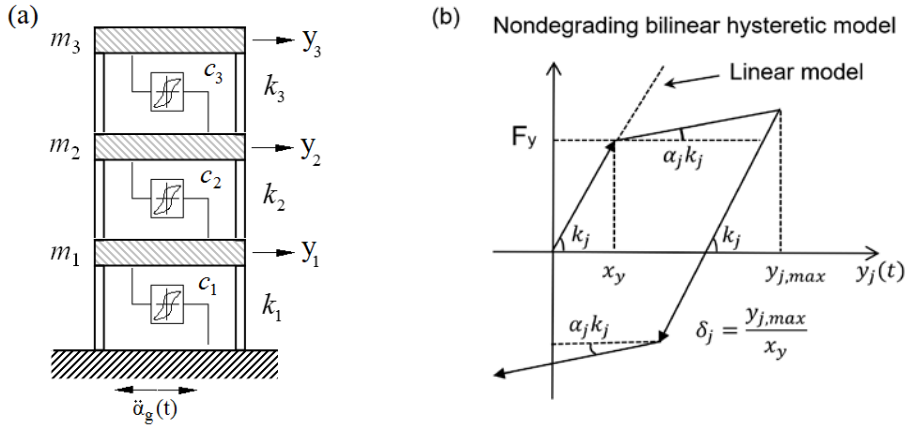

Fig. 3. (a) The three-story nonproportionally damped elastoplastic shear frame, and (b) the governing bilinear hysteretic restoring force-deformation law and definition of ductility ratio δ_j

3.2 System response amplitude process probability density functions

Following the efficient nonlinear stochastic dynamics technique delineated in sections 2.2-2.4, higher order statistics (i.e. the PDF) for the nonlinear response amplitude processes are efficiently determined. Note that the proposed method retains the particular advantageous property of obtaining reliable approximate estimation of the response considering only the first few modes which capture the majority of the system energy. Nevertheless, in the herein study the total number of the available modes is considered. In this regard, the response amplitude process PDFs arise as the outcome of the convolution of the involved distributions given in Eq.(34) multiplied by the associated modal participation factors Γ_{ji} corresponding to the

participation of every mode in the estimation of the response amplitude process PDF $p(A_j, t)$ of the *j*-th DOF of the system.

The achieved level of accuracy for the proposed technique is presented in Figs. 4a-b by comparing proposed methodology results with pertinent MCS data involving a large ensemble of 1000 acceleration time-histories generated compatibly with the specifications provided in Figs. 2a and 2b respectively. The employed stationarity assumption draws its credibility from the fact that the herein study possess a reliability assessment perspective, thus the interest is justifiably focused on a specific t_{cr} when $e(t; M_m, r)$ takes its highest value; this attribute enables the underlying stochastic seismic processes to be assumed as locally stationary in time.

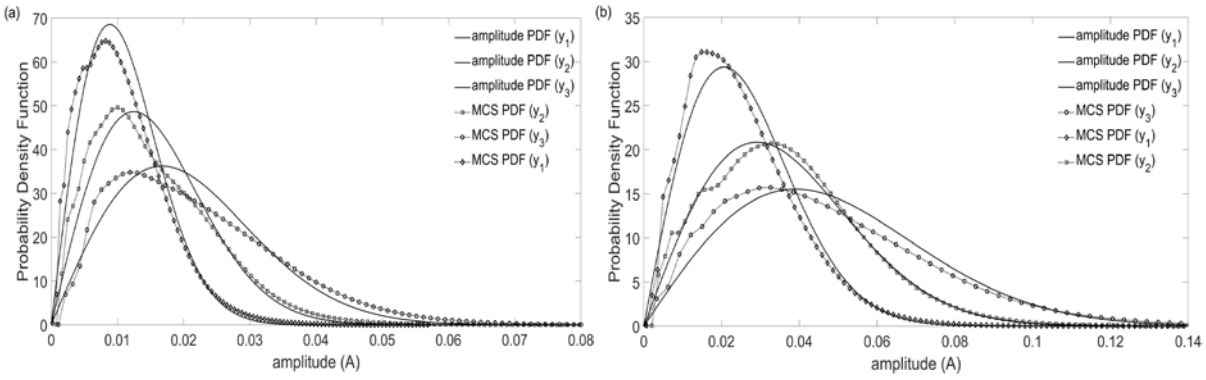

Fig. 4. Response amplitude process PDFs of the elastoplastic three-story shear frame exposed to seismic excitation process characterized by magnitude-epicentral distance earthquake properties shown in (a) Fig. 2a and (b) Fig. 2b. Comparison with Monte Carlo data (1000 realizations).

Evidently, comparisons with MCS data reveal a satisfactory degree of accuracy for excitations defined for different magnitude-epicentral distance earthquake properties. This observation renders the proposed technique appropriate for response determination purposes and related performance-based engineering applications at a low computational cost.

3.3 Efficient fragility surface estimates and assessment via nonlinear RHA

Seismic fragilities serve as a quantitative measure of the structural system vulnerability. Notably, the limit states fragility surfaces are determined at a minimum computational cost, harnessing the potential of the developed efficient fragility analysis methodology outlined in section 2. Proposed methodology-based results are compared with nonlinear RHA within a Monte-Carlo simulation context utilizing an ensemble of 1000 artificial acceleration time-histories compatible with the power spectrum of the underlying stochastic process for specific magnitude-epicentral distance earthquake properties using the spectral representation method [33]. Next, the nonlinear differential equations of motion in Eq.(9) are numerically integrated via a standard fourth order Runge-Kutta scheme, and finally, system response statistics as well as system fragilities are obtained based on the ensemble of the response realizations.

The fragility surfaces determined via the proposed fragility analysis methodology are compared with the corresponding MCS data. Specifically, in Figs. 5a and 5b the fragility surfaces corresponding to the limit state of *Moderate structural damage* are provided. Pertinent results for the totality of the considered limit states can be found in the subsequent Figs. 5c-h.

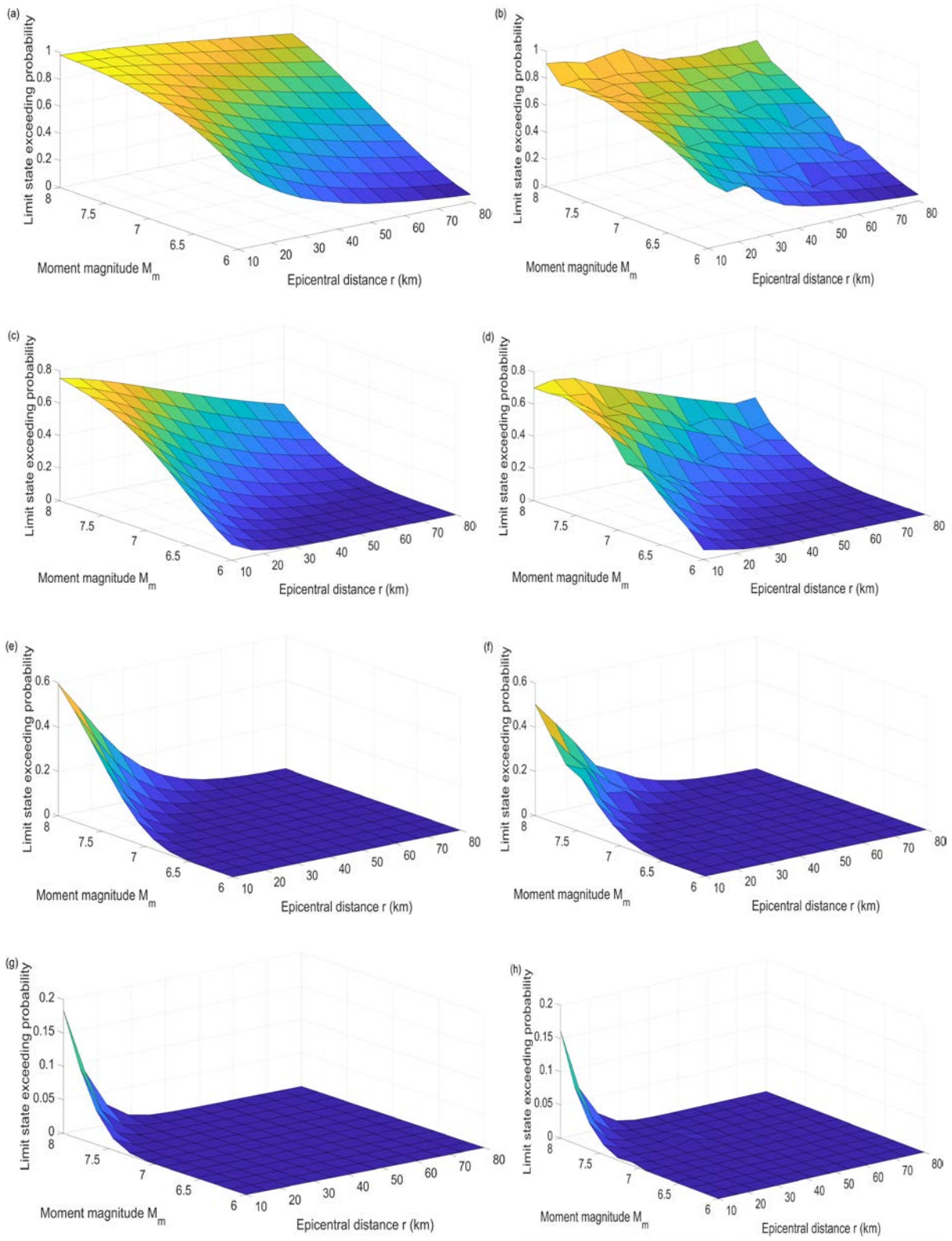

Fig. 5. Fragility surface estimates of the three-story elastoplastic shear frame shown in Fig. 3a for the limit state *Moderate structural damage* (a) via the proposed methodology (b) via MCS, for the limit state *Impaired function* (c) via the proposed methodology (d) via MCS, for the limit state *Life safety*

(e) via the proposed methodology (f) via MCS, and, for the limit state *Onset of collapse* (g) via the proposed methodology (h) via MCS.

Considering the pertinent results provided in Figs. 5a-h, it is noted that the achieved degree of accuracy is sufficient, since it provides with adequately accurate fragility estimates regardless the degree of the exhibiting nonlinearity among the DOFs of the system. It should be recalled that various values of α_j have been considered herein, reflecting nonlinear behaviors of different gradation. Based on the presented results, the proposed methodology evinces potential to address cases of larger complex nonlinear systems subject to hazards provided in spectral representation form. Further, the forced equivalent eigenvalues $\lambda_i^{eq}, \bar{\lambda}_i^{eq}$ based on the degree of the exhibiting nonlinearity provide a solid basis for interpreting the dynamic character of the system. Note that the proposed method leads to substantial reduction of the computational effort as compared with nonlinear RHA within a MCS framework. In this setting, to provide with an indicative order of magnitude for the computational cost involved, utilizing a laptop computer with standard configurations, the proposed technique needs 5-6 min, whereas the MCS based system fragilities estimation (1000 time-histories) requires 16–18 h.

It is noteworthy that an intersection over a limit state fragility surface along the moment magnitude axis leads to a form which bear high resemblance with the standard definition of fragility curves, typically encountered in the literature. Interestingly, an intersection along the epicentral distance provides with an alternative expression of fragility curves expressed also as function of the epicentral distance rather than a standard scalar intensity measure of the excitation (i.e. PGA). This observation confirms that the proposed fragility surfaces could be seen as an alternative useful counterpart of the standard fragility curves in the space domain. The low computational cost attribute hopefully qualifies the herein proposed approach as a potent analysis tool for preliminary seismic fragility analysis of yielding structures, without any restrictions on the nature of the damping matrices (e.g. such problems fairly arise in equipment-structure-type systems). It is worth mentioning that the seismic demands are imposed by an assigned stochastic seismological model, thus, the proposed approach can readily be modified to handle specifications prescribed by various stochastic models representing any kind of hazard (e.g. winds, ocean-waves, hurricanes etc).

4 CONCLUDING REMARKS

This paper proposes an efficient fragility analysis methodology which encompasses a novel inelastic modal decomposition method for random vibration analysis in alignment with specifications prescribed by an advanced point source stochastic seismological model for determining the probability law of the induced ground motion considering non-classically damped and nonlinear MDOF systems. Relying on statistical linearization and state-variable formulation the complex eigenvalue problem is addressed. Next, utilizing the forced vibrational modal properties of the linearized MDOF system in conjunction with a stochastic averaging treatment, the MDOF system modal response amplitude process PDFs are determined. The modal participation factors are evaluated for the complex-valued mode shapes and the total response amplitude process PDFs are defined in physical coordinates. Lastly, appropriate damage/limit states are considered for assessing system related fragilities at a low

computational cost.

It is noteworthy that the proposed methodology provides with reliable higher order statistics of the selected engineering demand parameter rather than simple estimates only of the mean and the standard deviation currently being the norm in the literature. Further, the associated low computational cost renders the proposed methodology particularly useful for efficient system fragility analysis and related performance-based engineering design applications.

The concepts involved have been numerically illustrated using a three-storey bilinear hysteretic frame structure exposed to ground motion modeled in the form of a non-homogenous stochastic field. Lastly, nonlinear response time-history analysis involving a large ensemble of acceleration time-histories has been conducted to assess the accuracy of the proposed framework in a Monte Carlo-based context.

ACKNOWLEDGEMENTS

The research work herein was supported by the German Research Foundation under Grant No. BE 2570/7-1 and MI 2459/1-1. This support is gratefully acknowledged.

REFERENCES

[1] Spanos P.D., Vargas Loli L.M., A statistical approach to generation of design spectrum compatible earthquake time histories, *Soil Dynamics & Earthquake Engineering, 4(1), 2-8, 1985.*

[2] Boore D. M., Simulation of ground motion using the stochastic method, *Journal of Pure Applied Geophysics; 160:635-676, 2003.*

[3] T. H. Caughey and M. E. J. OKelly, Classical normal modes in damped linear dynamic systems, *J. appl. mech. ASME 32,583-588, 1965.*

[4] Igusa T., Der Kiureghian A., Sackman J.L., Modal decomposition method for stationary response of non-classically damped systems, *Earthquake Engineering and Structural Dynamics; Vol. 12, 121-136, 1984.*

[5] Roberts J.B., Spanos P.D., *Random vibration and statistical linearization*, New York: Dover Publications, *2003*.

[6] Li J., Chen J., *Stochastic dynamics of structures*. John Wiley and Sons; 2009.

[7] Mitseas I. P., Beer M., Modal decomposition method for response spectrum based analysis of nonlinear and non-classically damped systems, *Mechanical Systems and Signal Processing, vol. 131: 469–485, 2019.*

[8] Tubaldi E., Barbato M., Dall' Asta A., Performance-based seismic risk assessment for buildings equipped with linear and nonlinear viscous dampers, *Engineering Structures 78, 90-99, 2014.*

[9] Mitseas, I.P., Kougioumtzoglou, I.A., Beer, M. An approximate stochastic dynamics approach for nonlinear structural system performance-based multi-objective optimum design. *Structural Safety*; vol. 60, p. *67-76, 2016.*

[10] Mitseas, I.P., Kougioumtzoglou, I.A., Spanos P.D., Beer, M. Nonlinear MDOF system Survival Probability Determination Subject to Evolutionary Stochastic Excitation. *Journal of Mechanical Engineering; 62 7-8, 440-451, 2016.*

[11] Der Kiureghian A., Fujimura K., Nonlinear stochastic dynamic analysis for performance-based earthquake engineering, *Earthquake Engineering and Structural Dynamics; 38:719–738, 2009.*

[12] Kafali C., Grigoriu M., Seismic fragility analysis: Application to simple linear and nonlinear systems, *Earthquake Engineering and Structural Dynamics; 36: 1885-1900, 2007.*

[13] Rezaeian S., Der Kiureghian A., A stochastic ground motion model with separable temporal and spectral nonstationarities, *Earthquake Engineering and Structural Dynamics; 37:1565–1584, 2008.*

[14] Vlachos C., Papakonstantinou K. G., Deodatis G. A multi-modal analytical non-stationary spectral model for characterization and stochastic simulation of earthquake ground motions, *Soil Dynamics and Earthquake Engineering, vol. 80, pp. 177-191, 2016.*

[15] Atkinson G.M., Silva W., Stochastic modeling of California ground motions, *Bullet SeismologSoc Am; 90(2):255-74, 2000.*

[16] Aki K., Generation and Propagation of G Waves from the Niigata Earthquake of June 16, 1964. Part 2. Estimation of Earthquake Moment, Released Energy, and Stress-strain Drop from the G-Wave Spectrum, *Bull. Earthq. Res. Inst. 44, 73–88, 1966.*

[17] Hanks T. C., Kanamori H., A moment magnitude scale, *J. Geophys. Res. B, 84, 2348-2350, 1979.*

[18] Au S. K., Beck J. L., Subset simulation and its application to seismic risk based on dynamic analysis, *Journal of Engineering Mechanics (ASCE); 129:901–917, 2003*.

[19] Taflanidis A. A, Beck J. L. Life-cycle cost optimal design of passive dissipative devices. *Structural Safety; 31:508–22, 2009*.

[20] Gidaris I., Taflanidis A. A Performance assessment and optimization of fluid viscous dampers through life-cycle cost criteria and comparison to alternative design approaches, *Bull Earthquake Eng; 13:1003–1028, 2015*.

[21] Sinha R., Igusa T. CQC and SRSS methods for non-classically damped structures, *Earthquake Engineering and Structural Dynamics; Vol. 24, 615-619, 1995*.

[22] Mitseas I. P., Kougioumtzoglou I. A., Giaralis A., Beer M. A novel stochastic linearization framework for seismic demand estimation of hysteretic MDOF systems subject to linear response spectra, *Structural Safety;* vol. 72: 84-98, *2018*.

[23] Chopra A.K., Chintanapakdee C. Inelastic deformation ratios for design and evaluation of structures: single-degree-of-freedom bilinear systems. *J Struct Eng ASCE; 130:1309–19, 2004*.

[24] Suzuki Y, Minai R. Application of stochastic differential equations to seismic reliability analysis of hysteretic structures. *Probabilistic Engineering Mechanics;3: 43–52, 1988*.

[25] Caughey T.K. Random excitation of a system with bilinear hysteresis. *J Appl Mech ASME; 27:649–52, 1960*.

[26] Kougioumtzoglou I. A., Spanos P. D., Nonlinear MDOF system stochastic response determination via a dimension reduction approach, *Computers and Structures; 126: 135-148, 2013.*

[27] Mitseas I. P., Kougioumtzoglou I. A., Spanos P. D., Beer M., Reliability assessment of nonlinear MDOF systems subject to evolutionary stochastic excitation, *Proceedings of the 7th International Conference on Computational Stochastic Mechanics (CSM 7), Santorini, Greece, 15-18 June, 2014, doi: 10.3850/978-981-09-5348-5_042*.

[28] Spanos P. D., Lutes L. D, Probability of response to evolutionary process, J. *Eng Mech. Div. Am. Soc. Civil Eng., 106, 213-224, 1980.*

[29] Ellingwood BR., Earthquake risk assessment of building structures, *Reliab. Eng. Syst. Saf.;74: 251–62, 2001*.

[30] Chopra A.K., Dynamics of Structures, Global Edition, Pearson, 2015.

[31] Grigoriu M., To Scale or Not to Scale Seismic Ground-Acceleration Records, *Journal of Engineering Mechanics;137:284-293, 2011*.

[32] Grigoriu M. Do seismic intensity measures (IMs) measure up?, *Probabilistic Engineering Mechanics; 46:80–93, 2016.*

[33] Shinozuka M., Deodatis G., Simulation of stochastic processes by spectral representation, Applied Mechanics Reviews 1991, vol. 44, no. 4, pp. 191-204.